

## Theory of nuclear-induced spectral diffusion: Spin decoherence of phosphorus donors in Si and GaAs quantum dots

Rogerio de Sousa and S. Das Sarma

*Condensed Matter Theory Center, Department of Physics, University of Maryland, College Park, Maryland 20742-4111, USA*

(Received 27 November 2002; published 29 September 2003)

We propose a model for spectral diffusion of localized spins in semiconductors due to the dipolar fluctuations of lattice nuclear spins. Each nuclear spin flip flop is assumed to be independent, the rate for this process being calculated by a method of moments. Our calculated spin decoherence time  $T_M=0.64$  ms for donor electron spins in Si:P is a factor of 2 longer than spin echo decay measurements. For  $^{31}\text{P}$  nuclear spins we show that spectral diffusion is well into the motional narrowing regime. The calculation for GaAs quantum dots gives  $T_M=10-50$   $\mu\text{s}$  depending on the quantum dot size. Our theory indicates that nuclear induced spectral diffusion should not be a serious problem in developing spin-based semiconductor quantum computer architectures.

DOI: 10.1103/PhysRevB.68.115322

PACS number(s): 03.67.Lx, 76.30.-v, 76.60.Lz, 85.35.Be

### I. INTRODUCTION

Electron and nuclear spins in semiconductors are promising qubit candidates for quantum computation because their intrinsic quantum two level nature together with existing semiconductor microelectronics technology can potentially satisfy the strict control and scalability requirements of a quantum computer (QC). Hence electron spins in quantum dots (QD's) (Ref. 1) and donor impurities<sup>2</sup> as well as nuclear spins in semiconductors<sup>3</sup> have been suggested as candidate building blocks for feasible QC architectures.<sup>4</sup> However, to build such a device major advances in single spin manipulations are needed, and for this purpose realistic calculations of semiconductor spin dynamics are essential to guide the experimental effort currently taking place. A question of particular importance is whether a localized spin will remain unaffected by the many interactions invariably present in a semiconductor environment during a time interval long enough for fault tolerant quantum computation (equivalent to  $10^4-10^6$  quantum gating times.<sup>5</sup>) In a recent paper<sup>6</sup> we showed that spin coherence of bound electronic states in semiconductors is limited by spin-spin interactions at low temperatures. When this interaction is between the qubits themselves, it can in principle be incorporated into the QC Hamiltonian, although this will lead to more complicated gate sequences. In particular we are not aware of any theoretical QC work specifically working out such gate sequences incorporating interqubit interactions. Therefore it is instructive to analyze the error introduced by ignoring some of these interactions, as we did in the case of dipolar coupled spin qubits.<sup>6</sup> The presence of many nonresonant spins in the system, such as lattice nuclei, also leads to phase fluctuation of the spin qubit, an effect which is hard to control. This has been denoted spectral diffusion (SD) since the qubit Zeeman frequency will diffuse through the spin resonance line. Spectral diffusion specifically refers to fluctuations in the Zeeman frequency  $\gamma B_{\text{eff}}=g\mu_B B_{\text{eff}}/\hbar$  (where  $g$  is the effective  $g$  factor,  $\mu_B=e\hbar/2mc$  the Bohr magneton, and  $B_{\text{eff}}$  the effective local magnetic field) of the electron due to external effects arising from the semiconductor environment. Note that such

fluctuations could arise either because the effective magnetic field  $B_{\text{eff}}$  is changing dynamically or because the electron  $g$  factor is varying. There are many physical processes leading to spectral diffusion, and here we are specifically interested in the limiting processes at the lowest temperatures. The physical process of interest to us is therefore dipolar nuclear fluctuations.

The first order of magnitude estimate of this effect was applied to Si:P donor electrons,<sup>17</sup> while our recent paper<sup>6</sup> used the same methods to estimate the SD rate in GaAs QD's. However, these estimates assumed *a priori* that nuclear pairs flipfopped slowly (and hence the echo decay was  $\sim \exp(-\tau^3)$ ) with a rate given by an unjustified phenomenological equation [Eq. (15) in Ref. 17 and Eq. (8) in Ref. 6]. Here we propose a description for this decoherence mechanism, arising from dipolar fluctuations of the lattice nuclear spins, affecting the qubit Zeeman frequency through hyperfine coupling. Even though we still treat each nuclear pair as an independent Markovian random variable (an approximation which seems reasonable for temperatures well above nuclear dipolar ordering, happening on the nK scale), our theory describes fast and slow flip flops on the same footing incorporating motional narrowing effects previously absent in former treatments (which happens when the fluctuation is so fast that SD is suppressed). We also derive microscopic expressions for these flip-flop rates, leading to a more refined calculation of nuclear SD for GaAs QD's and Si:P donor electrons, together with a treatment of this effect for a  $^{31}\text{P}$  donor nucleus.

In the case of localized spins precessing in a magnetic field  $B$ , knowledge of three phenomenological parameters is sufficient to describe the spin 1/2 dynamics: The gyromagnetic ratio  $\gamma$  which determines the precessing frequency (or equivalently the  $g$  factor  $g=2mc\gamma/e$ , with  $e$  the electronic charge,  $m$  the bare electron mass, and  $c$  the speed of light), the longitudinal relaxation time or spin-flip time  $T_1$ , and finally the transverse relaxation time or dephasing time  $T_2$ , which is often denoted coherence time since it sets the time scale of coherent superpositions between states along the  $B$  field direction.<sup>7</sup> However, electron spins in a solid state en-

environment often have different precession frequencies, either due to hyperfine fields from nearby nuclear spins or from unequal gyromagnetic ratios (arising, for example, from varying carrier effective mass). Therefore the transverse magnetization of a spin ensemble will decay in a time scale  $T_2^*$  which is in general much shorter than the single spin dephasing time  $T_2$ . The latter time scale can be measured using a  $\pi/2-\pi$  spin echo sequence.<sup>8</sup> The time it takes for this echo to decay to  $1/e$  of its initial value conveniently defines our single spin coherence time and has been historically called  $T_M$  (spin memory time)<sup>9</sup> since the echo envelope usually does not decay exponentially as predicted by the Bloch equations from which  $T_2$  was first defined.<sup>7</sup> (In Appendix B we show that measuring a  $\pi/2-\pi$  echo is equivalent to measuring the modulus squared of a single spin off diagonal density matrix element.)

It has been known for a very long time that SD caused by nearby nonresonant spins is usually the dominant echo decay mechanism.<sup>10</sup> However, all former SD theories assumed a *single* relaxation rate for the nonresonant spins, an approximation perfectly suitable for “ $T_1$  samples,” whereby these spins change their states through spin flips only. The theories of Herzog and Hahn,<sup>10</sup> and later Klauder and Anderson,<sup>11</sup> described the central spin Zeeman frequency as a random variable evolving in time according to Gaussian and Lorentzian conditional probabilities, respectively. These assumptions lead to a  $\pi/2-\pi$  echo decay of the form  $\exp(-2T_1^{-1}\delta^2\tau^3/3)$  and  $\exp(-T_1^{-1}\delta\tau^2)$ , respectively, as long as  $\tau \ll T_1$ , with  $2\tau$  being the time interval between the first pulse and the echo. Both  $\delta$  ( $t \rightarrow \infty$  linewidth for the conditional probabilities) and  $T_1$  (spin-flip time of nonresonant spins) are parameters that can, in principle, be calculated from the interactions. If the condition  $\tau \gg T_1$  is satisfied, one obtains  $\exp(-T_1\delta^2\tau)$  and  $\exp(-\delta\tau)$ , respectively, characterizing the motional narrowing regime. Interestingly, Gaussian SD correctly describes motional narrowing since  $T_1$  appears in the numerator, but Lorentzian SD does not, the decay being independent of  $T_1$ . Motivated by this inadequacy of the Lorentzian theory, Zhidomirov and Salikhov<sup>12</sup> proposed a many parameter model, which treated the number of flips of a spin  $i$  during a time interval  $t$  as a Poisson random variable parametrized by  $t/T_1$ , the frequency change on the central spin being  $\Delta_i$ . Their theory obtained the correct motional narrowing limit and agreed with experiment in dilute  $T_1$  samples where the nonresonant spins are randomly distributed. Our problem, however, is in a completely different regime. Here SD is caused by Si and GaAs lattice nuclei, which have  $T_1$  of the order of hours and hence the relevant time scale is given by the dipolar interaction, which varies substantially depending on the specific pair flip flopping (such a system is denominated a “ $T_2$  sample,” since  $T_2 \ll T_1$  for the spins that create the SD effect). We generalize the latter theory<sup>12</sup> to many relaxation rates  $T_{nm}^{-1}$ , each corresponding to a pair  $n, m$  of nuclear spins. We also present a microscopic theory to calculate these flip-flop rates. Altogether this approach is, to our knowledge, the first systematic attempt to describe SD in  $T_2$  samples. We also show that our

theory reduces to the earlier simple approximations of Refs. 6,11 in the appropriate limits.

The phosphorus donor impurity in silicon is the textbook example of a localized electron spin in a semiconductor. It has been extensively studied experimentally using electron spin resonance (ESR) (Refs. 13–15) and successful theories for its gyromagnetic ratio and  $T_1$  were developed.<sup>15,16</sup> However  $T_M$  for P in Si remained unexplained, even though it was measured thirty years ago.<sup>17</sup> Our model leads to a  $T_M$  two times longer than the measured value (this agreement should be considered reasonable since existing theories for  $T_1$  are also off by a factor of 2<sup>15,16</sup>). Our theory predicts a smooth transition of the echo envelope from Gaussian SD to motional narrowing behavior, this transition being well described by a correlation function. If the echo decay of <sup>31</sup>P donor nuclei is measured, we predict an echo envelope purely exponential, well into this motional narrowing regime, with  $T_M=0.60$  s. An important point discussed here is how SD is rapidly suppressed by reducing the amount of nuclear magnetic moments in the lattice. Our calculations show that isotopic purification of Si (exchanging spin- $1/2$  <sup>29</sup>Si nuclei by spin-0 <sup>28</sup>Si) may lead to coherence times as long as 100 ms for P impurities in Si, a result supported by recent experiments.<sup>18</sup> Unfortunately, Ga and As nuclei have no stable spin-0 isotopes, hence it seems that the only way to increase spin coherence in these materials is to suppress flip-flop events by nuclear polarization, as can, for example, be done by applying a strong external magnetic field or by using the Overhauser effect. Furthermore, we recently reported  $T_M$  calculations for a GaAs quantum dot.<sup>6</sup> This was particularly important since  $T_M$  has never been measured in this system, and a realistic assessment of the feasibility of a quantum dot quantum computer was needed. The detailed calculation presented here confirms our previous estimates. Hence the present paper together with other recent calculations of  $g$  factor<sup>19</sup> and  $T_1$  (Ref. 20) available in the quantum dot literature provides a general picture for electron spin dynamics in these heterostructures.

It is instructive to clarify the relationship between our results and recently published theories<sup>21</sup> on related issues. In Ref. 21 the authors considered a Hamiltonian which contained only hyperfine couplings between a single electron and the lattice nuclei, discarding the essential ingredient of the spectral diffusion effect, which is the dipolar interaction between nuclei. Hence their mechanism is based on flip flops between electron and nuclear spins. But when a  $B$  field is applied electron-nuclear flip flops are forbidden by energy conservation, since the nuclear Zeeman energy is  $10^3$  times smaller than the electronic Zeeman splitting. Therefore their mechanism is only relevant at low  $B$  fields, when the hyperfine coupling is of the same magnitude or greater than the electronic Zeeman energy, leading to the condition  $B \leq \hbar \gamma_I |\Psi(0)|^2 \ll 100$  G, where  $\gamma_I$  is the nuclear gyromagnetic ratio and  $|\Psi(0)|^2 = 10^{22} - 10^{25} \text{ cm}^{-3}$  is the electron's probability density on a nucleus. The theory presented here is valid in the opposite limit  $B \gg 100$  G.

This paper is organized in two parts: General theory and applications. In the first part (Sec. II) we describe our theory of spectral diffusion due to a dipolar coupled spin system.

This general theory can be easily applied to other spin resonance experiments, such as three pulse echoes. In the next part (Sec. III) we give numerical results for three particular cases, and discuss their implications for the current experimental effort in semiconductor spin quantum computation. We conclude in Sec. IV with a summary and some general comments.

## II. GENERAL THEORY

### A. Stochastic theory for the nuclear bath

Our problem is to describe the dynamics of a carrier spin  $\mathbf{S}$  coupled to a lattice of nuclear spins  $\mathbf{I}_n$ . The total Hamiltonian can be separated into three parts:  $\mathcal{H} = \mathcal{H}_S + \mathcal{H}_{SI} + \mathcal{H}_I$ ,

$$\mathcal{H}_S = \gamma_S B S_z, \quad (1)$$

$$\mathcal{H}_{SI} = \sum_n A_n I_{nz} S_z, \quad (2)$$

$$\begin{aligned} \mathcal{H}_I = & -\gamma_I B \sum_n I_{nz} - 4 \sum_{n < m} b_{nm} I_{nz} I_{mz} \\ & + \sum_{n < m} b_{nm} (I_{n+} I_{m-} + I_{n-} I_{m+}), \end{aligned} \quad (3)$$

$$\begin{aligned} A_n = & \gamma_S \gamma_I \hbar \left\{ \frac{8\pi}{3} |\Psi(\mathbf{R}_n)|^2 \right. \\ & \left. - \int d^3r |\Psi(\mathbf{r})|^2 \frac{|\mathbf{r} - \mathbf{R}_n|^2 - 3[(\mathbf{r} - \mathbf{R}_n) \cdot \hat{\mathbf{z}}]^2}{|\mathbf{r} - \mathbf{R}_n|^5} \right\} \\ & \approx \gamma_S \gamma_I \hbar \left\{ \frac{8\pi}{3} |\Psi(\mathbf{R}_n)|^2 - \frac{1 - 3 \cos^2 \theta_n}{|\mathbf{R}_n|^3} \theta(|\mathbf{R}_n| - r_0) \right\}, \end{aligned} \quad (4)$$

$$b_{nm} = -\frac{1}{4} \gamma_I^2 \hbar \frac{1 - 3 \cos^2 \theta_{nm}}{R_{nm}^3}. \quad (6)$$

Here the Hamiltonians are divided by  $\hbar$  to simplify the notation;  $\gamma_S$  and  $\gamma_I$  are gyromagnetic ratios,  $A_n$  the coupling with a nucleus located at position  $\mathbf{R}_n$ ,  $\mathbf{R}_{nm}$  the relative vector between two nuclei, and  $\theta_{nm}$  the angle between this vector and the  $B$  field direction. The electron-nucleus coupling  $A_n$  includes a hyperfine term and a residual dipolar interaction. The hyperfine term comes from the singularity of the integral [Eq. (4)], which is removed by integrating over the angular coordinates first. Here we will assume this dipolar term is only effective for  $|\mathbf{R}_n| > r_0$ , which is a proper length scale for the electron's wave function ( $\theta$  is the step function, while  $\theta_n$  the angle between  $\mathbf{R}_n$  and the  $B$  field). The nuclear spins are in constant turmoil due to their mutual dipolar interaction. To see how this affects the spin  $S$  we approximate each nuclear spin operator  $2I_{nz}$  by a classical random variable  $\sigma'_n(t) = \pm 1$ , which is valid only if the nuclei have spin  $1/2$  (this description is still accurate for spin  $I > 1/2$ , as long

as the nuclei are in the slow SD regime, see below). Hence the Zeeman frequency  $\omega_z$  of the electron spin becomes

$$\omega_z(t) = \gamma_S B + \frac{1}{2} \sum_n A_n \sigma'_n(t). \quad (7)$$

On the other hand, the evolution of the nuclei is strongly affected by the field produced by the central spin  $S$ . This effect is treated by assuming the nuclei evolve according to the effective Hamiltonian

$$\mathcal{H}'_I = \mathcal{H}_I + \frac{1}{2} \sum_n A_n I_{nz}, \quad (8)$$

which conserves total spin in the  $z$  direction. Therefore when any  $I_{nz}$  flips, a corresponding  $I_{mz}$  must flop in the opposite direction. These flip-flop events show that we cannot treat the random variables  $\sigma'_n$  as independent of each other. Rather, we will treat pairs of spins as independent random variables. Hence Eq. (7) becomes

$$\omega_z(t) = \sum_{n < m} \Delta_{nm} \sigma_{nm}(t) + \text{const}, \quad (9)$$

with  $\Delta_{nm} = |A_n - A_m|/2$ , and  $\sigma_{nm} = \pm 1$  random variables uncorrelated with each other. We further make the Markovian assumption that the probability that  $\sigma_{nm}$  changes sign during a time interval  $t$  is given by  $t/T_{nm}$ , independent of past values of  $\sigma_{nm}$  (this Markovian approximation is reasonable in the absence of any contrary evidence about the stochastic fluctuations of the nuclear spins). Hence the number of flip flops  $N(t)$  is a Poisson random variable with parameter  $t/T_{nm}$ , and we may write

$$\sigma_{nm}(t) = \sigma_{nm}(0) (-1)^{N(t)}, \quad (10)$$

with  $N(t)$  having the distribution

$$P(N(t) = k) = \frac{1}{k!} \left( \frac{t}{T_{nm}} \right)^k \exp\left(-\frac{t}{T_{nm}}\right). \quad (11)$$

In the next section we show how to calculate the flip-flop rate  $T_{nm}^{-1}$ .

We now proceed to the derivation of the spin echo decay. The complex in-plane magnetization

$$v(t) = \langle S_x \rangle + i \langle S_y \rangle, \quad (12)$$

can be calculated for any spin echo sequence by taking the average<sup>10,11</sup>

$$v(t) = \left\langle \exp\left( i \int_0^t s(t') \omega_z(t') dt' \right) \right\rangle. \quad (13)$$

For the  $\pi/2 - \pi$  echo considered here the echo function  $s(t) = 1$  for  $0 \leq t < \tau$  and  $s(t) = -1$  for  $\tau \leq t$ . Therefore

$$v(t) = \prod_{n < m} v_{nm}(t), \quad (14)$$

$$v_{nm}(t) = \left\langle \cos\left[ \Delta_{nm} \int_0^t s(t') (-1)^{N(t')} dt' \right] \right\rangle, \quad (15)$$

where we take an average over  $\sigma_{nm}(0) = \pm 1$  with probability 1/2 [this average applies to an ensemble of spins; however, we show in Appendix B that the effect of the echo is precisely to remove this average, making  $v(t)$  exactly equal to a single spin in-plane magnetization]. In Appendix A we calculate this average, and the result is<sup>22</sup>

$$v_{nm}(t) = \theta(\tau - t)v_{nm}^{(F)}(t) + \theta(t - \tau)v_{nm}^{(E)}(t), \quad (16)$$

$$v_{nm}^{(F)}(t) = \exp\left(-\frac{t}{T_{nm}}\right) \left[ \frac{1}{R_{nm}T_{nm}} \sinh(R_{nm}t) + \cosh(R_{nm}t) \right], \quad (17)$$

$$v_{nm}^{(E)}(t) = R_{nm}^{-2} \exp\left(-\frac{t}{T_{nm}}\right) \left\{ \frac{1}{T_{nm}^2} \cosh(R_{nm}t) + \frac{R_{nm}}{T_{nm}} \sinh(R_{nm}t) - \Delta_{nm}^2 \cosh[R_{nm}(t - 2\tau)] \right\}, \quad (18)$$

with  $R_{nm}^2 = T_{nm}^{-2} - \Delta_{nm}^2$ . We distinguish two limits in the above expressions: For nuclear pairs causing fast spectral diffusion, consider  $T_{nm}^{-1} \gg \Delta_{nm}$ . In that case we have

$$v_{nm}^{(E)}(t) \approx v_{nm}^{(F)}(t) \approx \exp\left(-\frac{1}{2} \Delta_{nm}^2 T_{nm} t\right) + \mathcal{O}(\Delta_{nm}^2 T_{nm}^2), \quad (19)$$

which shows that fast flip-flopping nuclei do not even form an echo. Rather, they contribute to a ‘‘motional narrowed’’ signal,<sup>8</sup> which decays exponentially in a time scale that lengthens as  $T_{nm}^{-1}$  increases. The idea is that the echo sequence can not refocus the spins if their Zeeman frequency changes appreciably over  $\tau$ . For large  $T_{nm}^{-1}$  the nuclear pair contributes to a homogeneously broadened line, not an echo peak.<sup>12</sup> The slow SD limit  $T_{nm}^{-1} \ll \Delta_{nm}$  implies

$$v_{nm}^{(E)}(t) = \exp\left(-\frac{t}{T_{nm}}\right) \left\{ \cos[\Delta_{nm}(t - 2\tau)] + \frac{1}{\Delta_{nm}T_{nm}} \sin(\Delta_{nm}t) \right\} + \mathcal{O}(\Delta_{nm}^{-2} T_{nm}^{-2}). \quad (20)$$

After performing the product over these slow nuclear pairs, Eq. (14) will have a peak at  $t \approx 2\tau$ . This is because if  $t \neq 2\tau$ , the argument of the product will be zero for some pair  $n, m$  making the whole product vanish. Assuming the echo peak occurs exactly at  $2\tau$ , we get

$$v_{nm}^{(E)}(2\tau) \approx \exp\left\{-\frac{1}{T_{nm}} \left[ 2\tau - \frac{\sin(2\Delta_{nm}\tau)}{\Delta_{nm}} \right]\right\}. \quad (21)$$

If in addition to this slow spectral diffusion regime, we look at the limit  $\Delta_{nm}\tau \ll 1$ , the result is

$$v_{nm}^{(E)}(2\tau) \approx \exp\left[-\frac{1}{6} \frac{\Delta_{nm}^2}{T_{nm}} (2\tau)^3\right], \quad (22)$$

which is very similar to an expression derived previously by us<sup>6</sup> using Gaussian spectral diffusion as a starting point.

Apart from a factor of 2 these expressions differ by a term which takes into account the small broadening due to spin-flip processes. Since this term was introduced heuristically and only changes numerical values by a negligible amount we will not include it here.

Notice that nothing should be concluded about the qualitative decay of  $v(2\tau)$  before performing the product over pairs in Eq. (14). For example, in the particular case of SD caused by dilute paramagnetic impurities ( $\Delta_{nm} \sim r^{-3}$  with  $r$  being the impurity-electron distance) it can be shown that  $v(2\tau) \sim \exp(-a\tau - b\tau^2)$ <sup>12</sup> after calculating Eq. (14) and taking a spatial average. Indeed exactly this behavior was seen in the electron spin echo decay of Si:P when the P concentration was high enough such that spectral diffusion due to nearby nonresonant electrons was dominant.<sup>17</sup> Here we deal with even more complicated expressions for  $\Delta_{nm}$  [our Eqs. (57), (62), and (67)]. Moreover it is often the case that  $T_{nm}^{-1} \sim \Delta_{nm}$  and use of the limits (19), (21) becomes unjustified. Hence in our calculations below we perform the product (14) using the exact expressions (18).

Finally, it is easy to calculate the correlation function [see Eq. (A4)]

$$\chi_c(t) = \lim_{t' \rightarrow 0} \frac{\langle \omega(t)\omega(t') \rangle - \langle \omega(t) \rangle \langle \omega(t') \rangle}{\langle \omega^2(t') \rangle - \langle \omega(t') \rangle^2} \quad (23)$$

$$= \sum_{n < m} P_{nm} \exp\left(-\frac{2t}{T_{nm}}\right), \quad (24)$$

$$P_{nm} = T_{nm}^{-1} \Delta_{nm}^2 / \sum_{i < j} T_{ij}^{-1} \Delta_{ij}^2. \quad (25)$$

The averages in Eq. (23) assume  $\sigma_{nm}(t=0) = +1$  for all pairs  $n, m$ . Then  $\chi_c(t_c) = e^{-1}$  defines the correlation time for the effect of the nuclear bath on the spin  $S$ . While the two parameter Gaussian SD theory has a simple exponential correlator  $\chi_c = \exp(-t/T_1)$ , Eq. (24) in general does not decay exponentially. This correlator makes clear the difference between our many parameter ( $T_{nm}, \Delta_{nm}$ ) stochastic theory and these simpler theories. If  $t \ll t_c$ , we will have  $\chi_c(t) \sim 1$ , each  $\sigma_{nm}(t)$  performing less than one flip flop on average. Below we show numerically that this regime leads to  $v_E(2\tau) \sim \exp(-\tau^3)$ . Therefore, when our calculated  $T_M \ll t_c$ , we predict a Gaussian SD decay for the echo. However, when  $T_M \gg t_c$ ,  $\chi_c(T_M) \ll 1$  indicating that most  $\sigma_{nm}$  have already performed many flip flops. In this case we obtain  $v_E(2\tau) \sim \exp(-\tau)$ , characterizing a motional narrowing regime since the nuclear bath dynamics may be considered fast. Therefore the importance of our correlation function is to describe the transition to motional narrowing induced by all nuclear pairs, not just a single one satisfying  $T_{nm}^{-1} \gg \Delta_{nm}$ .

It is important to discuss the case of general nuclei with spin  $I > 1/2$ , where Eq. (10) does not apply. Then  $\sigma(t)$  will be a random walk variable with equal probabilities of moving right or left,

$$\sigma(t) = 2I\Delta, (2I-2)\Delta, \dots, -2I\Delta. \quad (26)$$



Of course for  $I > 1/2$  we cannot represent  $\sigma(t)$  as an analytical function of the number of steps  $N(t)$ . However, for small  $t$  [such that  $\chi_c(t) \approx 1$ , or  $tT_{nm}^{-1} \ll t\Delta_{nm} \ll 1$ ] Eq. (22) will still hold, since  $\sigma(t)$  will take at most one step (of length  $2\Delta$ ). We will use this fact when considering GaAs nuclei, which have  $I = 3/2$  (see below).

### B. Calculating the nuclear flip-flop rates

We now show how to calculate the rate  $T_{nm}^{-1}$  appearing in Eq. (18), for dipolar coupled spin  $I$  nuclei. As noted above, we will assume the nuclear dynamics to be decoupled from the central spin  $S$  through the effective Hamiltonian  $\mathcal{H}'_I$ , Eq. (8). Furthermore, we will separate  $\mathcal{H}'_I$  in a secular part  $\mathcal{H}_0$  and flip-flop terms  $F_{nm}(t)$  which contain an harmonic time dependence

$$\mathcal{H}'_I = \mathcal{H}_0 + \sum_{n < m} F_{nm}(t), \quad (27)$$

$$\mathcal{H}_0 = - \sum_n \left( \gamma_I B - \frac{1}{2} A_n \right) I_{nz} - 4 \sum_{n < m} b_{nm} I_{nz} I_{mz}, \quad (28)$$

$$F_{nm}(t) = b_{nm} (I_{n+} I_{m-} + I_{n-} I_{m+}) \cos(\omega t), \quad (29)$$

where we have introduced a fictitious frequency variable  $\omega$  for theoretical convenience—eventually we are interested in the  $\omega = 0$  limit. We shall see that it is useful to introduce the frequency  $\omega$ : The rate  $T_{nm}^{-1}$  will be obtained by taking the  $\omega \rightarrow 0$  limit. Suppose we have  $N$  nuclear spins  $\mathbf{I}_n$ . We will label the eigenstates of  $\mathcal{H}_0$  by the index  $a = 0, 1, \dots, 2^N$ :  $\mathcal{H}_0|a\rangle = E_a|a\rangle$ . Obviously we simply have  $|a\rangle = |m_1 m_2 \dots m_N\rangle$  with  $m_i = \pm 1/2$ . The transition rate between two of these states induced by  $F_{nm}(t)$  is then given by Fermi's golden rule to be

$$\mathcal{W}_{a,b}^{n,m} = \frac{\pi}{2} b_{nm}^2 |\langle a|F_{nm}|b\rangle|^2 [\delta(E_a - E_b - \omega) + \delta(E_a - E_b + \omega)], \quad (30)$$

with  $F_{nm} = (I_{n+} I_{m-} + I_{n-} I_{m+})$ . The central spin phase changes by  $\Delta_{nm} = |A_n - A_m|/2$  during one of these events. Moreover, we will assume the nuclei in thermal equilibrium, each state  $|a\rangle$  populated with a Boltzmann probability

$$p(a) = \exp\left(-\frac{E_a}{k_B T}\right) / \sum_b \exp\left(-\frac{E_b}{k_B T}\right). \quad (31)$$

Then the flip-flop rate for a pair  $nm$  becomes

$$T_{nm}^{-1}(\omega) = \sum_{a,b} p(a) \mathcal{W}_{a,b}^{n,m}. \quad (32)$$

At zero temperature  $p(a)$  will be nonzero only for the ground state. Furthermore, if  $B \gg b_{nm}/\gamma_I I \sim 0.1$  G this ground state will simply be  $|0\rangle = |I, I, \dots, I\rangle$ , and  $T_{nm}^{-1} = 0$  for all pairs  $nm$ , leading to vanishing zero temperature decoherence. However, nuclear Zeeman energies are only  $\sim 1$  mK/T, much lower than typical dilution refrigerator

temperatures ( $\geq 10$  mK). Hence a reasonable approximation is to assume  $k_B T \gg \hbar \gamma_I B$ , and  $p(a) = (2I+1)^{-N}$  for all states  $|a\rangle$ . This in fact makes Eq. (32) much easier to calculate, particularly since we will employ a technique similar to the method of moments due to Van Vleck.<sup>8,23</sup> Therefore we assume  $p(a)$  to be the same for all states  $a$ , and rewrite Eq. (32) in the form

$$T_{nm}^{-1}(\omega) = 2\pi b_{nm}^2 \rho_{nm}(\omega), \quad (33)$$

with  $\rho_{nm}(\omega)$  playing the role of a density of states given by

$$\rho_{nm}(\omega) = \frac{1}{2(2I+1)^N} \sum_{a,b} |\langle a|F_{nm}|b\rangle|^2 \delta(E_a - E_b - \omega). \quad (34)$$

The invariance of the trace operation allows us to calculate any moment of  $\rho_{nm}(\omega)$  exactly. We define the  $n$ th moment as

$$\langle \omega^n \rangle = \int_0^\infty \omega^n \rho_{nm}(\omega) d\omega / \int_0^\infty \rho_{nm}(\omega) d\omega. \quad (35)$$

As an example of how to calculate these moments, consider the normalization constant

$$\begin{aligned} \mathcal{A}(I) &= \int_0^\infty \rho_{nm}(\omega) d\omega \\ &= \frac{1}{4(2I+1)^N} \sum_{a,b} \langle a|F_{nm}|b\rangle \langle b|F_{nm}|a\rangle \\ &= \frac{1}{4(2I+1)^N} \text{Tr}\{F_{nm}^2\} \\ &= \frac{2}{15} \frac{I(I+1)}{2I+1} [2I(I+1)+1]. \end{aligned} \quad (36)$$

It is straightforward to prove the following relations:

$$\langle \omega \rangle = \bar{\omega} = 2\mathcal{C}(I) \text{Tr}\{[\mathcal{H}_0, F_{nm}] I_{n+} I_{m-}\} = \frac{1}{2} |A_n - A_m|, \quad (37)$$

$$\mathcal{C}(I) = \frac{15}{8} \frac{(2I+1)^{-N+1}}{I(I+1)[2I(I+1)+1]}, \quad (38)$$

$$\langle \omega^2 \rangle = -\mathcal{C}(I) \text{Tr}\{[\mathcal{H}_0, F_{nm}]^2\}, \quad (39)$$

$$\langle (\omega - \bar{\omega})^2 \rangle = \frac{16}{3} I(I+1) \sum_{i \neq n,m} (b_{ni} - b_{mi})^2, \quad (40)$$

$$\langle \omega^4 \rangle = \mathcal{C}(I) \{[\mathcal{H}_0, [\mathcal{H}_0, F_{nm}]]^2\}, \quad (41)$$

$$\begin{aligned} \langle (\omega - \bar{\omega})^4 \rangle &= \frac{2^8}{3} I(I+1) \left\{ -\frac{1}{5} [2I(I+1)+1] \right. \\ &\quad \times \sum_{i \neq n,m} (b_{ni} - b_{mi})^4 + I(I+1) \\ &\quad \left. \times \left[ \sum_{i \neq n,m} (b_{ni} - b_{mi})^2 \right]^2 \right\}. \end{aligned} \quad (42)$$

Using these expressions we can discuss various possibilities for the shape of  $\rho_{nm}(\omega)$ , which is clearly an even function of  $\omega$  with peaks at  $\pm|A_n - A_m|/2$ . The most common choice in line shape theory is to assume each peak to be a Gaussian or a Lorentzian with a cutoff at the wings.<sup>8</sup> To decide between these, we define a dimensionless parameter

$$\xi_{nm} = \frac{\langle(\omega - \bar{\omega})^4\rangle}{3\langle(\omega - \bar{\omega})^2\rangle^2} = 1 + \left(\frac{1-3f}{3f}\right) \frac{\sum_{i \neq n,m} (b_{ni} - b_{mi})^4}{\left[\sum_{i \neq n,m} (b_{ni} - b_{mi})^2\right]^2}. \quad (43)$$

Here we have introduced the occupation probability  $f$  for a nucleus at site  $i$  (sums involving one site and two sites are proportional to  $f$  and  $f^2$ , respectively). For a Gaussian function this ratio would be exactly 1. For a Lorentzian, it would be equal to  $\sim \alpha_{nm}/\delta_{nm} \gg 1$ , where  $\alpha_{nm}$  is the cutoff and  $\delta_{nm}$  the halfwidth at half maximum. Clearly  $f \ll 1$  leads to Lorentzian rates. Here we will adopt the following approximation: Whenever  $\xi_{nm} \leq 10$  we will approximate  $\rho_{nm}(\omega)$  by a Gaussian; if  $\xi_{nm} > 10$  we will use the Lorentzian fit. The Gaussian approximation leads to

$$\rho_{nm}(\omega) = \mathcal{A}(I) \frac{1}{\sqrt{2\pi\kappa_{nm}}} \left\{ \exp\left[-\frac{(\omega - \bar{\omega})^2}{2\kappa_{nm}^2}\right] + \exp\left[-\frac{(\omega + \bar{\omega})^2}{2\kappa_{nm}^2}\right] \right\}, \quad (44)$$

with

$$\kappa_{nm} = \sqrt{\langle(\omega - \bar{\omega})^2\rangle}. \quad (45)$$

The desired flip-flop rate is then obtained by setting  $\omega=0$  in Eqs. (44) and (33),

$$T_{nm}^{-1}(\xi_{nm} \leq 10) = 2\sqrt{2\pi}\mathcal{A}(I) \frac{b_{nm}^2}{\kappa_{nm}} \exp\left(-\frac{|A_n - A_m|^2}{8\kappa_{nm}^2}\right). \quad (46)$$

For  $\xi_{nm} > 10$  we assume the Lorentzian form

$$\rho_{nm}(\omega) = \mathcal{A}(I) \frac{\delta_{nm}}{\pi} \left[ \frac{\theta(\omega - \bar{\omega} + \alpha_{nm}) - \theta(\omega - \bar{\omega} - \alpha_{nm})}{\delta_{nm}^2 + (\omega - \bar{\omega})^2} + \frac{\theta(\omega + \bar{\omega} + \alpha_{nm}) - \theta(\omega + \bar{\omega} - \alpha_{nm})}{\delta_{nm}^2 + (\omega + \bar{\omega})^2} \right], \quad (47)$$

with  $\theta$  being the step function. It is important to note that this Lorentzian must have a cutoff so that its second and higher moments do not diverge. The parameters  $\alpha_{nm}$  and  $\delta_{nm}$  can be easily related to Eqs. (40) and (42):

$$\delta_{nm} \approx \frac{\pi}{2\sqrt{3}} \sqrt{\frac{\langle(\omega - \bar{\omega})^2\rangle^3}{\langle(\omega - \bar{\omega})^4\rangle}}, \quad (48)$$

$$\alpha_{nm} \approx \sqrt{\frac{2\langle(\omega - \bar{\omega})^4\rangle}{\langle(\omega - \bar{\omega})^2\rangle}}. \quad (49)$$

The Lorentzian flip-flop rate is

$$T_{nm}^{-1}(\xi_{nm} > 10) = 4\mathcal{A}(I) \frac{b_{nm}^2}{\delta_{nm}} \frac{1 - \theta(|A_n - A_m| - 2\alpha_{nm})}{1 + [(A_n - A_m)/(2\delta_{nm})]^2}. \quad (50)$$

Therefore  $T_{nm}^{-1}$  will be suppressed unless  $|A_n - A_m| \leq \kappa_{nm}, \delta_{nm}$ . This effect stems from energy conservation: For a flip flop to happen, an amount  $|A_n - A_m|/2$  of energy must be absorbed by the dipolar term in  $\mathcal{H}_0$ . To see this consider two states with  $I = 1/2$ ,  $|a\rangle = |1/2, -1/2, m_3, \dots, m_N\rangle$ ,  $|b\rangle = |-1/2, +1/2, m_3, \dots, m_N\rangle$ . Their energy difference is

$$E_a - E_b = \frac{1}{2}(A_1 - A_2) - 4 \sum_{i \neq 1,2} (b_{1i} - b_{2i})m_i. \quad (51)$$

If we calculate the average square of this expression using  $\langle m_i^2 \rangle = 1/4$ ,  $\langle m_i \rangle = 0$  we get

$$\langle (E_a - E_b)^2 \rangle = \left(\frac{A_1 - A_2}{2}\right)^2 + 4 \sum_{i \neq 1,2} (b_{1i} - b_{2i})^2, \quad (52)$$

showing that an adjustment of the spin system can supply energies up to  $\sim \kappa_{nm}$  to compensate for the central spin field. We believe that the above expressions for  $T_{nm}^{-1}$  are considerably more precise than the phenomenological rates used in the earlier literature without any derivations.<sup>6,17,24</sup>

### III. APPLICATIONS

#### A. Electron spin of a phosphorus donor in silicon

We now turn to applications of our theory for systems of interest to quantum computation in spin-qubit-based semiconductor architectures. We start by considering the electron spin of a shallow donor in silicon. In natural samples, 95.33% of silicon atoms have no nuclear magnetic moment.<sup>25</sup> Those are the <sup>28</sup>Si isotopes. Spectral diffusion is then caused by the remaining fraction  $f_{\text{nat}} = 0.0467$  of <sup>29</sup>Si isotopes which are spin 1/2 nuclei with gyromagnetic ratio  $\gamma_i^{\text{Si}} = 5.31 \times 10^3$  (s G)<sup>-1</sup>. These nuclei will produce a hyperfine field on the electron donor impurity given by Eq. (5), which is proportional to the electron's probability density at the nuclear site  $\mathbf{R}_n$ ,  $|\Psi(\mathbf{R}_n)|^2$ . For this state we assume the Kohn-Luttinger wave function<sup>13,26</sup>

$$\Psi(\mathbf{r}) = \frac{1}{\sqrt{6}} \sum_{j=1}^6 F_j(\mathbf{r}) u_j(\mathbf{r}) e^{i\mathbf{k}_j \cdot \mathbf{r}}, \quad (53)$$

$$\mathbf{k}_j = 0.85 \frac{2\pi}{a_{\text{Si}}} \hat{k}_j, \quad \hat{k}_j \in \{\hat{x}, -\hat{x}, \hat{y}, -\hat{y}, \hat{z}, -\hat{z}\}, \quad (54)$$

$$F_{1,2}(\mathbf{r}) = \frac{\exp\left[-\sqrt{\frac{x^2}{(nb)^2} + \frac{y^2 + z^2}{(na)^2}}\right]}{\sqrt{\pi(na)^2(nb)}}, \quad (55)$$

with the appropriate corresponding envelope functions  $F_j$  [Eq. (55)] with anisotropies in the  $y$  and  $z$  directions. Here  $n = (0.029 \text{ eV}/E_i)^{1/2}$  with  $E_i$  being the ionization energy of the impurity ( $E_i = 0.044 \text{ eV}$  for the phosphorus impurity, hence  $n = 0.81$  in our case),  $a_{\text{Si}} = 5.43 \text{ \AA}$  the lattice parameter for Si,  $a = 25.09 \text{ \AA}$  and  $b = 14.43 \text{ \AA}$  characteristic lengths for Si hydrogenic impurities.<sup>13</sup> Moreover, we will use experimentally measured values for the charge density on each Si lattice site<sup>26,27</sup>

$$|u_j(\mathbf{R}_n)|^2 = \eta \approx 186. \quad (56)$$

Hence the hyperfine interaction is given by

$$A_n = \frac{16\pi}{9} \gamma_S^{\text{Si}} \gamma_I^{\text{Si}} \hbar \eta [F_1(\mathbf{R}_n) \cos(k_0 X_n) + F_3(\mathbf{R}_n) \cos(k_0 Y_n) + F_5(\mathbf{R}_n) \cos(k_0 Z_n)]^2 - \gamma_S^{\text{Si}} \gamma_I^{\text{Si}} \hbar \frac{1 - 3 \cos^2 \theta_n}{|\mathbf{R}_n|^3} \theta(|\mathbf{R}_n| - na), \quad (57)$$

with  $k_0 = (0.85)2\pi/a_{\text{Si}}$ , and  $\gamma_S^{\text{Si}} = 1.76 \times 10^7 \text{ (s G)}^{-1}$  the gyromagnetic ratio for the electron donor. It is instructive to check the experimental validity of Eq. (57) by calculating the inhomogeneous linewidth ( $\sim 1/\gamma_S^{\text{Si}} T_2^*$ ). A simple statistical theory applied to Eq. (7) leads to<sup>26</sup>

$$\langle (\omega/\gamma_S^{\text{Si}} - B)^2 \rangle = \frac{f}{(2\gamma_S^{\text{Si}})^2} \sum_{\mathbf{R}_n \neq 0} A_n^2. \quad (58)$$

For  $f = 0.0467$  our calculated root mean square linewidth is equal to 0.89 G. On the other hand, an ESR scan leads to  $2.5 \text{ G}/2\sqrt{2 \ln 2} = 1.06 \text{ G}$ .<sup>13</sup> Therefore our model is able to explain 84% of the experimental hyperfine linewidth [the residual dipolar term in Eq. (57) only contributes  $\sim 0.1\%$  to this linewidth].

Before discussing our spin echo decay results we should mention how the  $^{29}\text{Si}$  fraction  $f$  enters our calculations. For example, Eq. (14) becomes

$$v(2\tau) = \prod_{n < m} [v_{nm}(2\tau)]^{f^2}, \quad (59)$$

since the probability of a pair  $n, m$  to be  $^{29}\text{Si}$  is  $f^2$ . Also single and double sums in Eqs. (40) and (42) are proportional to  $f$  and  $f^2$  (these sums are calculated assuming the pair  $n, m$  is already occupied; hence the question is whether or not site  $i \neq n, m$  contains a  $^{29}\text{Si}$ ). To perform our numerical calculations we take the natural logarithm of Eq. (59). Then we take advantage of the fact that  $b_{nm} \propto R_{nm}^{-3}$  [Eq. (6)] decays fast as a function of the inter-nuclear distance  $R_{nm}$ . Therefore we achieve faster convergence by summing over lattice sites  $n$  together with some of its close neighbors  $m$ . Both the range of sites  $n$  and the number of neighbors included in the sum were increased systematically to ensure proper convergence. From the convergence check we concluded that summing within eight characteristic lengths of the wave function ( $\sim 40a_{\text{Si}}$  for the Si:P case) plus including up to six nearest neighbor shells gave excellent convergence.

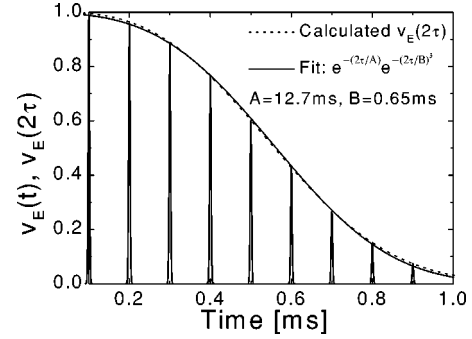


FIG. 1. Calculated echo peaks  $v_E(t)$  and echo envelope  $v_E(2\tau)$  as a function of time for a single donor electron spin in Si:P. We assumed the Si lattice had natural abundance of  $^{29}\text{Si}$  ( $f = 0.0467$ ) and  $B \parallel [111]$ . We also show a fit for our echo envelope that compares well with the experimental fit of Ref. 17 [see Eq. (60)].

Figure 1 shows the echo signal [Eq. (18)] as a function of time for natural Si and  $B \parallel [111]$ . Clearly the echoes occur at  $t = 2\tau$ . The echo envelope, defined by the maximum of each peak, should be compared with the empirical experimental fit of Chiba and Hirai,<sup>17</sup>

$$v_{\text{exp}}(2\tau) = \exp \left[ - \left( \frac{2\tau}{0.6 \text{ ms}} \right) - \left( \frac{2\tau}{0.4 \text{ ms}} \right)^3 \right]. \quad (60)$$

Clearly our theory is able to explain quite successfully the  $\exp(-\tau^3)$  decay, but our exponential tail is twenty times smaller than the measured value. Therefore our theory suggests this extra exponential decay is coming from other decoherence mechanisms, perhaps related to imperfections of the ESR pulses. [Recent experimental data<sup>18</sup> suggest dipolar scattering between donor electrons is responsible for the extra exponential decay seen in Eq. (60).] Nevertheless, our  $T_M = 0.64 \text{ ms}$  is  $\sim 2$  times larger than the measured value of 0.3 ms, a quite good agreement in view of former spin relaxation calculations.<sup>14</sup> Including the residual dipolar term in  $A_n$  [see Eq. (57)] changes  $T_M$  by less than 1%, showing that here SD is dominated by flipflopping nuclei inside the electron's wave function [if we set the hyperfine term to zero in Eq. (57), we get  $T_M = 1.7 - 1.9 \text{ ms}$  for  $0 < r_0 \leq na$ ]. It is interesting to note that former SD estimates<sup>9,17</sup> neglected the hyperfine contribution, arguing that nuclei inside the electron's wave function could not flip flop due to the large  $\Delta_{nm}$  they would induce. Surprisingly, our calculation shows that this coupling is very important, although estimates using only the dipolar term would still lead to reasonable results. The hyperfine term becomes more and more important as the wave function size increases. Figure 2 shows the behavior of  $-\ln v_E(2\tau)$  for  $B \parallel [111]$  and a few values of  $f$ . As  $2\tau$  is increased, the echo envelope changes from a "Gaussian spectral diffusion" regime<sup>11</sup> [ $\sim \tau^3$ , well described by Eq. (22)] to  $-\ln v \sim \tau$  [see Eq. (19) and (21) for  $\Delta_{nm} \tau \gg 1$ ]. The "experimental window"  $0.1 \leq -\ln v \leq 3$  falls within this crossover for many values of  $f$ , including natural isotopic abundance. The exponential behavior obtained for long  $2\tau$  can be understood by looking at the correlation function [Eq. (24)] which also appears in Fig. 2 (right scale). Notice that this correlation function decays smoothly over 3 time de-

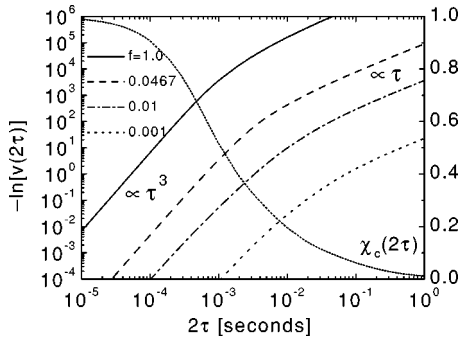


FIG. 2. The left scale shows the logarithm of the  $\pi/2-\pi$  echo envelope as a function of  $2\tau$  for electron spins of Si:P. For all  $^{29}\text{Si}$  isotopic fractions  $f$  this function undergoes a crossover from Gaussian spectral diffusion behavior [ $v \sim \exp(-k\tau^3)$ ] to motional narrowing [ $v \sim \exp(-k\tau)$ ]. The correlation function  $\chi_c(2\tau)$  is shown on the right scale; motional narrowing behavior corresponds to small values of  $\chi_c$ . This correlation function shows non-exponential decay, quite distinct from former theories<sup>6,10,11</sup> (see also Fig. 9 below). Here we have  $B \parallel [111]$ .

acades, but its behavior is clearly nonexponential (see Fig. 9), making evident the difference between our current complete theory and former heuristic ones based on the two parameter Gaussian conditional probability.<sup>6,10,11</sup> The small correlation between Zeeman frequencies before and after the application of the  $\pi$  pulse explains this motional narrowing behavior for  $v(2\tau)$  (see discussion at the end of Sec. II A). Note that Fig. 2 suggests it might be more appropriate to fit  $-\ln v(2\tau)$  to a function which approaches  $\tau$  at long times and  $\tau^3$  at short time scales. Such a fit could possibly yield a better description for experimental data as long as other contributing mechanisms (electron-electron dipolar scattering<sup>6</sup> for example) are properly subtracted.

It is interesting to see if the Si sixfold degeneracy embedded into the Kohn-Luttinger state [Eq. (53)] has a strong effect on  $T_M$ . We obtain  $T_M \sim 0.3$  ms at natural abundance using a hydrogenic state with Bohr radius  $\sim 20$  Å. Therefore we can conclude that the strong oscillations of  $A_n$  reduce  $T_{nm}^{-1}$  by a small amount, hence increasing  $T_M$  (as  $\Delta_{nm}$  is larger the energy cost for nuclear flip flops is higher). This gives an idea about the effect of the electron's field on the  $^{29}\text{Si}$  nuclei. Figure 3 shows  $T_M$  as a function of  $f$ . Only one purified sample with  $f = (0.12 \pm 0.08)\%$  was studied experimentally,<sup>28</sup> leading to  $T_M = 0.52$  ms. Note that this value is significantly different than what we have in Fig. 3 ( $\sim 0.1$  s) simply because at such low values of  $f$  the concentration of donors ( $4 \times 10^{16} \text{ cm}^{-3}$ ) lead to strong electron-electron dipolar scattering (see Fig. 2 of Ref. 6). It would be quite interesting to see spin echo measurements for different values of  $f$ , but as the isotopic purity increases one will have to decrease donor concentration significantly to ensure that dipolar scattering is not prevailing (for that purpose  $T_M$  should be independent of donor concentration, showing saturation for low P concentration<sup>17</sup>).

An interesting confirmation of our theory would be to measure  $T_M$  as a function of the  $B$  field tilting angle  $\theta$ . Figure 4 shows this angular dependence in samples with natural isotopic abundance.  $\theta = 0^\circ$  means  $B \parallel [001]$ , while  $\theta$

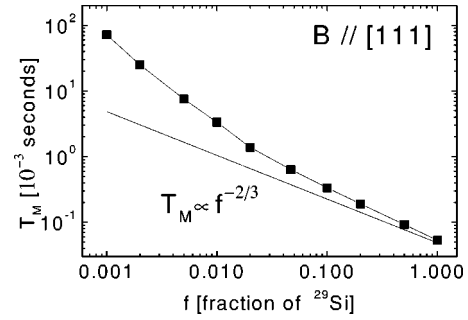


FIG. 3. Decoherence time ( $T_M$ ) of the Si:P electron spin as a function of  $^{29}\text{Si}$  content  $f$ . The straight line resembles a simple theory derived previously<sup>6</sup> where  $f$  only altered the flip-flop pair probability. Our theory deviates from this behavior since  $f$  also enters the moments [Eqs. (40) and (42)]. The change in slope seen in  $T_M$  is explained by the transition from Gaussian to Lorentzian flip flop expressions for  $T_{nm}^{-1}$  [see Eqs. (46) and (50)].

$= 90^\circ$   $B \parallel [110]$  (unfortunately Ref. 17 measured  $T_M$  only for  $B \parallel [111]$ ). Preliminary experimental data shows excellent qualitative agreement with Fig. 4.<sup>35</sup> Incidentally, our theory does not depend on the  $B$  field intensity, except for  $B \geq 10$  T: Then  $k_B T \gg \hbar \gamma_I B$  does not hold, and also the magnetic length  $l_B = (\hbar c / eB)^{1/2} \leq 20$  Å, and  $B$  is already deforming the electron's wave function. The latter effect does in fact appear in the quantum dot case, since its radius depends crucially on  $l_B$  [see Eq. (64)].

## B. Nuclear spin of a phosphorus donor in silicon

$^{31}\text{P}$  nuclear spins [ $\gamma_S^P = 1.08 \times 10^4$  (s G)<sup>-1</sup>] are promising qubit candidates when implanted in a Si matrix.<sup>3</sup> Its interaction with the lattice is rather weak, leading to a measured  $T_1 \sim 5$  h at  $B = 0.8$  T and  $T = 1.25$  K.<sup>14</sup> Here we calculate the contribution of  $^{29}\text{Si}$  spectral diffusion on the decoherence time  $T_M$  of an isolated  $^{31}\text{P}$  nucleus. There is an important difference between this calculation and the one related to the Si:P electron spin above. Even though the flip-flop rate of a pair  $n, m$  of  $^{29}\text{Si}$  ( $T_{nm}^{-1}$ ) is determined in exactly the same way as above [Eqs. (46) and (50) with  $A_n$  given by Eq. (57)], the corresponding phase change on the  $^{31}\text{P}$  spin is given by

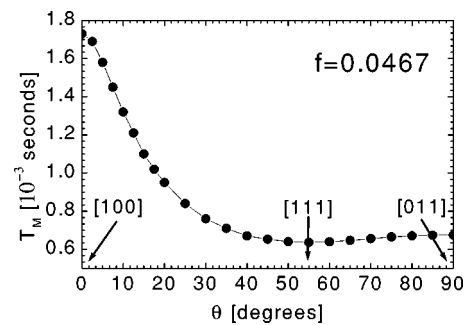


FIG. 4. Behavior of Si:P electron spin  $T_M$  as a function of  $B$  field tilting angle with respect to the crystal lattice for samples with natural abundance of  $^{29}\text{Si}$ . To our knowledge, this dependence has never been probed experimentally, and would be an interesting test for the accuracy of our theory.



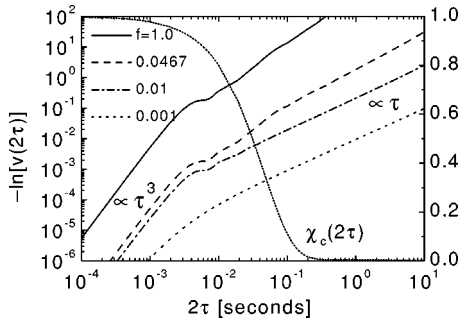


FIG. 5. Logarithm of  $\pi/2 - \pi$  echo envelope as a function of echo time  $2\tau$  for  $^{31}\text{P}$  nuclear spins in Si:P. This function undergoes an abrupt crossover from Gaussian spectral diffusion behavior to motional narrowing, quite different from the smooth transition seen on Fig. 2. On the right scale we plotted the correlation function  $\chi_c$ , which shows a sharper transition to motional narrowing as compared to Fig. 2 (here  $\chi_c$  changes over one time decade, as opposed to three in Fig. 2).

$$\Delta_{nm} = |A'_n - A'_m|/2, \quad (61)$$

$$A'_n = \gamma_S^P \gamma_I^{\text{Si}} \hbar \frac{1 - 3 \cos^2 \theta_n}{|\mathbf{R}_n|^3}, \quad (62)$$

where  $A'_n$  is the dipolar interaction between a  $^{29}\text{Si}$  nucleus located at  $\mathbf{R}_n$  and the  $^{31}\text{P}$  located at the origin (in principle we should include the effect of the  $^{31}\text{P}$  dipolar field on the flip-flop rates  $T_{nm}^{-1}$ , but we determined it to be negligible on the  $T_M$  calculation both in this section and the preceding one). It is easy to see that this phase change  $\Delta_{nm}$  is in most cases  $\sim 10^3$  smaller than the corresponding one for the electron. Therefore the motional narrowing condition  $T_{nm}^{-1} \gg \Delta_{nm}$  will be satisfied for many more pairs than in the last section. Hence we should expect  $v \sim \exp(-k\tau)$  for a wide range of parameters [see Eq. (19)].

Figure 5 shows the calculated shape of the echo envelope as a function of  $2\tau$ . The qualitative behavior is similar to Fig. 2 above, except for the rather abrupt crossover from Gaussian SD to motional narrowing behavior. For  $f \leq 0.0467$  the observed decay is indeed  $v \sim \exp(-k\tau)$  as predicted above. This behavior can be understood by looking at the correlation function  $\chi_c$  (right scale on Fig. 5) which goes to zero in only one time decade, evidencing the abrupt appearance of the motional narrowing regime. Unfortunately there are no experimental data available to verify this qualitative result. Figure 6 depicts the dependence of  $T_M$  as a function of  $f$ .

The dependence on the tilting angle  $\theta$  (Fig. 7) is significantly different than the one in Fig. 4. This can be explained by the fact that while in the former case first nearest-neighbor flip-flop dominated (about 92% of  $T_M^{-1}$ ), here first nearest neighbor amounts only to 3% of the rate, which is dominated by second nearest neighbors ( $\sim 90\%$  of  $T_M^{-1}$ ). This is why we see more oscillations in Fig. 6 than in Fig. 3: Second nearest neighbors are 12 in number, and have a more intricate lattice configuration than the four first nearest neighbors. Quite interestingly, in Fig. 7,  $T_M$  is maximized

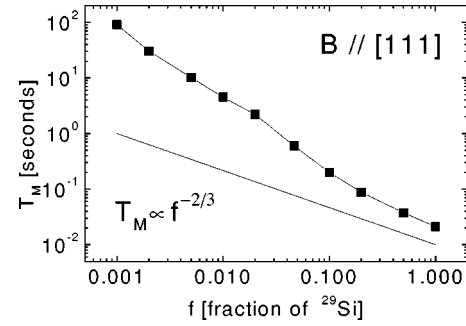


FIG. 6. Depicts  $T_M$  versus  $^{29}\text{Si}$  content  $f$  for  $^{31}\text{P}$  nuclear spins. Similar to Fig. 3, the change in slope around  $f \sim 0.01$  occurs due to the crossover to Lorentzian  $T_{nm}^{-1}$  [Eq. (50)].

when  $B$  points in the  $[110]$  direction, and displays a sharp peak in the  $[111]$  direction, while Fig. 4 shows  $T_M$  minimized when  $B$  points in both directions.

### C. Electron spin in a gallium arsenide quantum dot

Recent interest in the spin properties of a single electron GaAs QD is motivated by its potential use as a qubit.<sup>1,29</sup> One advantage over Si:P is the nondegenerate conduction band, with the minimum at the  $\Gamma$  point. Therefore the exchange interaction of a double dot is a smooth function of the inter-dot barrier and distance, quite different from two Si:P donors, where this exchange may oscillate dramatically as a function of donor separation.<sup>30</sup>

The GaAs lattice has a zinc-blende structure with 50% of  $^{75}\text{As}$ , 30.2% of  $^{69}\text{Ga}$ , and 19.8% of  $^{71}\text{Ga}$ .<sup>25</sup> These nuclei have spin  $I = 3/2$ , but here we present calculations using the spin  $1/2$  stochastic theory together with spin  $3/2$  flip-flop rates. Since the correlation function is very close to 1 in the neighborhood of our calculated  $T_M$ , the electron is well into the slow SD regime, making this approximation very accurate for our purpose. The electron hyperfine interaction with these nuclei will lead to an inhomogeneous linewidth of about 50 G for small dots (with Fock-Darwin radius  $\ell \sim 20$  nm; donor impurities in bulk GaAs have even higher broadening<sup>31</sup>). If one has an ensemble of these dots, the decoherence time  $T_M$  can be measured by using a  $\pi/2 - \pi$  pulse. However, ensembles of dots always contain size distribution. Since  $T_M$  will be quite sensitive to the radius  $\ell$

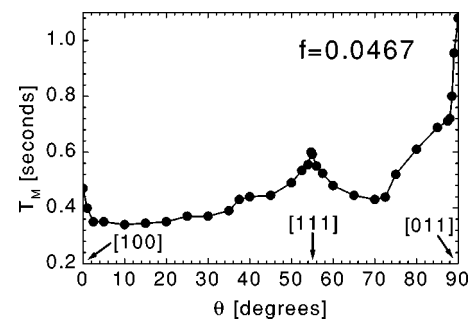


FIG. 7. Spectral diffusion decay time  $T_M$  versus  $B$  field tilting angle for  $^{31}\text{P}$  nuclei. This calculation assumes natural abundance of  $^{29}\text{Si}$ ,  $f = 0.0467$ .

(see below), it might be more appropriate to measure decoherence by applying an ESR field to a single dot and then measuring the signal using transport experiments, even though such experiments would only lead to a lower bound on  $T_M$ .<sup>32</sup>

The energy eigenstates of a quantum dot in the presence of spin-orbit coupling are a mixture of spin states up and down. Therefore if the electron spin is up, it will flip within a time  $T_1$  with the corresponding emission of a phonon. However, for the spin to flip a virtual transition to an excited orbital state has to happen, since spins do not couple directly to the phonon strain field. The result is a strong sensitivity on dot size and applied field  $B$ ,  $T_1^{-1} \propto \ell^8 B^5$ . For  $B \sim 1$  T and  $\ell \sim 30$  nm a recent theory leads to  $T_1 \sim 1$  ms, showing that for the small dots in a quantum computer architecture spin-flip scattering is strongly suppressed.<sup>20</sup> Recently we showed that the dominant decoherence mechanism in these small dots ( $\ell \lesssim 50$  nm) is nuclear spectral diffusion.<sup>6</sup> Here, our detailed calculation of this effect confirms the accuracy of the simple theory presented earlier,<sup>6</sup> justified by Eq. (22) and the fact that the correlation function [Eq. (24)] is still quite close to 1 in the neighborhood of  $T_M$ . For  $|z| \leq z_0/2$ , the quantum dot wave function can be simply approximated as

$$\Psi(\mathbf{r}) = \sqrt{\frac{2}{z_0}} \cos\left(\frac{\pi}{z_0} z\right) \frac{1}{\sqrt{\pi} \ell(B)} \exp\left(-\frac{x^2 + y^2}{2\ell^2(B)}\right), \quad (63)$$

and we assume  $\Psi = 0$  for  $z > z_0/2$ . This state is a reasonable description for the lowest orbital of a quantum well of thickness  $z_0$ , with electrostatic lateral parabolic confinement with radius  $\ell_0$ . The Fock-Darwin radius  $\ell(B)$  includes the additional  $B$  field confinement

$$\ell(B) = \frac{l_B l_0}{(l_B^4 + l_0^4/4)^{1/4}}, \quad (64)$$

$$l_B = \sqrt{\frac{\hbar c}{eB}}. \quad (65)$$

Then the hyperfine coupling  $A_n$  for a nucleus located at a coordinate  $(X_n, Y_n, Z_n)$  from the center of the dot becomes

$$A_n = \frac{16}{3} \frac{\gamma_S \gamma_I \hbar a_{\text{GaAs}}^3}{\ell^2(B) z_0} d(I) \cos^2\left(\frac{\pi}{z_0} Z_n\right) \exp\left(-\frac{X_n^2 + Y_n^2}{\ell^2(B)}\right) \times \theta(z_0/2 - |Z_n|) \quad (66)$$

$$- \gamma_S \gamma_I \hbar \frac{1 - 3 \cos^2 \theta_n}{|\mathbf{R}_n|^3} \theta[X_n^2 + Y_n^2 - \ell^2(B)]. \quad (67)$$

Here  $a_{\text{GaAs}} = 5.65$  Å,  $\gamma_S = -3.86 \times 10^6$  (sG)<sup>-1</sup> (assuming  $g = -0.44$  independent of  $\ell$  for the dot electron<sup>19</sup>),  $\gamma_I = 4.58, 8.16, 6.42 \times 10^3$  (sG)<sup>-1</sup>, and charge densities  $d(I) = 9.8, 5.8, 5.8 \times 10^{25}$  cm<sup>-3</sup> for <sup>75</sup>As, <sup>71</sup>Ga, and <sup>69</sup>Ga, respectively.<sup>33</sup> The residual dipolar coupling again leads to a very small correction (<1% of  $T_M$ ).

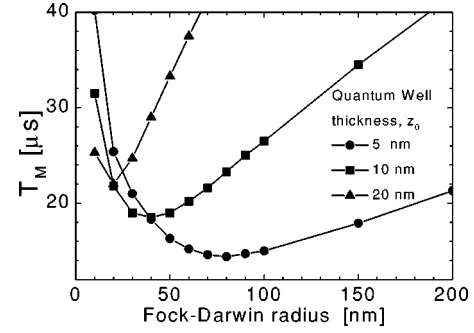


FIG. 8.  $T_M$  versus Fock-Darwin radius  $\ell$  for various quantum well thicknesses,  $z_0 = 5, 10, 20$  nm. Decoherence achieves a maximum as a function of  $\ell$ . Here  $B \parallel [111]$ .

Figure 8 shows the behavior of  $T_M$  as a function of Fock-Darwin radius  $\ell$  for three different quantum well thicknesses  $z_0$ . For each  $z_0$ ,  $T_M$  displays a minimum as a function of  $\ell$ . This arises from two competing effects: If we decrease the wave function size, fewer nuclei contribute to SD, hence  $T_M \rightarrow \infty$  as  $\ell \rightarrow 0$ . However when we increase  $\ell$  the wave function flattens, making two close pairs  $n, m$  produce similar hyperfine fields. Since it is the difference  $|A_n - A_m|$  which causes phase fluctuation,  $T_M \rightarrow \infty$  as  $\ell \rightarrow \infty$ . Therefore  $T_M$  must have a minimum as a function of the Fock-Darwin radius  $\ell$ . At this minimum,  $T_M \sim 10$  μs for all  $z_0$ . For all QD sizes considered here the SD decay is found to be  $\sim \exp(-\tau^3)$ , the correlation function being close to 1 in the neighborhood of  $T_M$  (Fig. 9). The dependence with  $\theta$  is similar to Fig. 4.

#### IV. CONCLUSION

We have developed a detailed quantitative theory for nuclear spectral diffusion of localized spins in semiconductors. By treating each nuclear pair independently, we are able to show that the echo signal arises from the interplay between fast and slow nuclear flip flops. The echo envelope undergoes a smooth transition from a Gaussian SD decay to an exponential motional narrowing when the nuclear bath loses correlation over time, this transition being well described by an appropriate correlation function. The Lorentzian approximation gives a good description of the intermediate crossover regime, and our theory gives a microscopic justification for the use of these phenomenological conditional probabilities. This behavior is quite general and should be observed in any decoherence mechanism where qubit phase fluctuation takes place. We apply our theory to three physical systems proposed as QC architectures, showing that SD should not be a decisive constraint in their development ( $T_M > 10$  μs; therefore  $T_M/\tau_J \gg 10^6$  for all architectures, where  $\tau_J$  is the time scale for the exchange gate<sup>6</sup>). Our calculated Si:P electron donor spin results agree well with existing experimental data for natural abundance of <sup>29</sup>Si, while  $T_M$  increases very fast as these isotopes are removed from the lattice. In addition our calculation shows that the most important contribution to SD comes from nuclei inside the electron's wave function spread, as opposed to electrons far away as was suggested before.<sup>17</sup> The <sup>31</sup>P nuclear spin is found to be in the motional narrowing regime, weakly af-

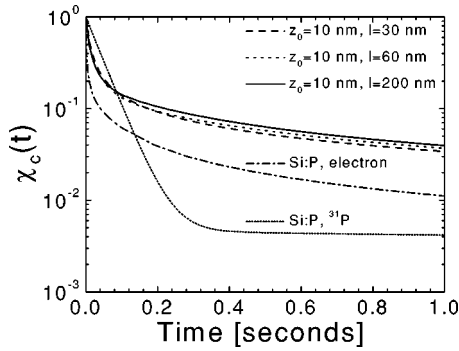


FIG. 9. Nonexponential decay of the correlation function  $\chi_c$  as a function of time [see Eq. (23)]. Initially  $\chi_c$  shows strong exponential decay, dominated by the fastest rate. Then slower processes take over. For Si:P we assume natural  $^{29}\text{Si}$  abundance, while  $B\parallel[111]$ . GaAs-QD's show a clear tendency to motional narrowing as  $\ell$  (Fock-Darwin radius) increases.

ected by  $^{29}\text{Si}$ . Our GaAs quantum dot calculations confirm our earlier estimates based on a simpler theory.<sup>6</sup> Although there are no Ga or As  $I=0$  isotopes, one way to reduce SD is to suppress flip-flop events by nuclear polarization. The main difference between  $T_1$  and  $T_2$  samples is the presence of several relaxation rates. This feature is evident in Fig. 9, where we show correlation functions for many cases treated here. Increasing QD radius  $\ell$  increases  $T_M$  and reduces  $\chi_c(T_M)$ , pushing large QD's to the motional narrowing regime. This result is clear evidence that SD does not affect delocalized states (such as conduction electrons), since all nuclear pairs will be in the motional narrowing regime [Eq. (19)].

We now briefly discuss the approximations assumed in our work. Certainly the most important one is that we treat nuclear pairs as independent Markovian processes, making random flip flops with a Poisson distribution. We believe this approximation is reasonable for a nuclear bath at temperatures much higher than its dipolar ordering critical temperature ( $\sim \hbar b_{nm}/k_B \sim 10^{-9}$  K), since in this case the spin correlation length can be assumed of the order of one lattice parameter. Of course this condition will always hold for dilution refrigerators (which operate at mK temperatures), and specially for the experiment discussed in this paper ( $T = 1.6$  K).<sup>17</sup> At high spin temperature the nuclear system undergoes frequent transitions through its  $(2I+1)^N$  available states. An important assumption implicit in our model is that only a subset of these transitions, namely, flip flops between close nuclear pairs [described by  $\sigma_{nm}$ , Eq. (9)] are responsible for the SD effect at external magnetic fields  $B \gg 100$  G. Four spin processes stem from higher order perturbations in Eq. (29), and can be neglected when  $b_{nm} \leq \Delta_{nm}$ , which is the case for the relevant nuclear pairs (otherwise, the condition  $b_{nm} \gg \Delta_{nm}$  immediately implies motional narrowing [see Eq. (19)] and this pair gives a negligible contribution to the SD rate). Preliminary experimental results<sup>35</sup> on the orientation dependence of  $T_M$  show excellent qualitative agreement with Fig. 4, suggesting the pair flip-flop picture is quite appropriate. One limitation of the uncorrelated pair approximation is that the echo peaks always occur at  $t=2\tau$ .

This happens because the product [Eq. (14)] will be zero away from  $2\tau$  as long as a single pair undergoes slow SD. A global treatment of all pairs such as the one achieved in the two parameter Gaussian theory leads to an echo peak formed between  $\tau$  and  $2\tau$ .<sup>11</sup> Nevertheless to our knowledge this effect does not seem to be present in  $\pi/2-\pi$  echo experiments,<sup>8,17</sup> our approximation being appropriate in this respect. Another approximation that seems reasonable is to neglect back action. We assume that the nuclei evolve under a static central spin field [Eq. (8)], unchanged by its effect on this spin.

Finally, we comment on the relationship between our current work and a number of other recent publications in the literature dealing with spin relaxation in the context of semiconductor quantum computer architectures.<sup>20,36,37</sup> We emphasize that our theory deals exclusively with electron spin decoherence *in the absence of any phonon effects*. Our work provides a theory for nuclear-induced spectral diffusion of (localized) electron spin in semiconductors, and as such we deal with electronic spin decoherence arising from the fluctuations induced by electron-nucleus hyperfine interactions caused by nuclear spin dipolar flip flops. Since the flip flops conserve nuclear energy, no phonons are required for the decoherence studied in this work.

Our work is a comprehensive theory for nuclear induced spectral diffusion in the spin decoherence of localized electrons in semiconductors—we do not invoke the empirical approximations and the heuristic arguments which were used to obtain earlier expressions for spectral diffusion existing in the literature.<sup>11,17,24</sup> As such our results are applicable and relevant not only to considerations involving solid state spin-qubit-based quantum computer architectures but also to all problems involving spin decoherence due to electron-nucleus hyperfine coupling where phonon effects are negligible (i.e., at low temperatures). In particular, our results apply to spin echo measurements in semiconductors at low temperatures, and it is therefore gratifying that we have been able to quantitatively explain hitherto unexplained Si spectral diffusion results of Ref. 17 dating back thirty years. We emphasize that our theory is still approximate since we are forced to make a number of approximations, the most important one being the assumption of uncorrelated flip flops among spin pairs. Although we believe this assumption of uncorrelated flip flops to be valid at “high” nuclear spin temperature ( $\gg$  nK), it is still worthwhile to consider further improvement of our theory by taking into account the full non-Markovian nature of the spin flip-flop processes in future work.

#### ACKNOWLEDGMENT

The authors acknowledge discussions with S.E. Barrett, A. Kaminski, S.A. Lyon, J. Fabian, and P. Zoller. This work is supported by ARDA, LPS, US-ONR, and NSF.

#### APPENDIX A: STOCHASTIC THEORY FOR A SINGLE FLIP-FLOPPING PAIR

The problem is to evaluate the average [Eq. (15)] for a single nuclear pair  $n,m$

$$v(t) = \left\langle \cos \left[ \Delta \int_0^t S(t') (-1)^{N(t')} dt' \right] \right\rangle, \quad (\text{A1})$$

with  $N(t)$  a Poisson random variable with parameter  $t/T$  (for simplicity we dropped the subscript  $nm$  from  $v_{nm}$ ,  $\Delta_{nm}$ ,  $T_{nm}$ ). Expanding the cosine and rearranging the product of integrals we get

$$v(t) = \sum_{k=0}^{\infty} (-1)^k \Delta^{2k} \int_0^t dt_{2k} S(t_{2k}) \int_0^{t_{2k}} dt_{2k-1} S(t_{2k-1}) \cdots \\ \times \int_0^{t_2} dt_1 S(t_1) \langle (-1)^\xi \rangle, \quad (\text{A2})$$

with  $\xi = N(t_1) + \cdots + N(t_{2k})$ . Using the inequality  $t \geq t_{2k} \geq t_{2k-1} \geq \cdots \geq t_1 \geq 0$  together with the fact that a sum of two Poisson variables with parameters  $t_i/T$  and  $t_j/T$  equals another Poisson with  $(t_i + t_j)/T$ , we get

$$\xi = N(t_{2k} - t_{2k-1}) + N(t_{2k-2} - t_{2k-3}) + \cdots + N(t_2 - t_1) \\ + 2[N(t_{2k-1}) + N(t_{2k-3}) + \cdots + N(t_1)], \quad (\text{A3})$$

$$\langle (-1)^\xi \rangle = \exp \left\{ -\frac{2}{T} [(t_{2k} - t_{2k-1}) \\ + (t_{2k-2} - t_{2k-3}) + \cdots + (t_2 - t_1)] \right\}, \quad (\text{A4})$$

since the number of flip flops  $N(t_{2k} - t_{2k-1})$  are assumed independent random variables for nonoverlapping time intervals  $t_{2k} - t_{2k-1}$  (Markovian approximation). Using Eqs. (A2) and (A4) we rewrite the echo decay in the form

$$v(t) = \sum_{k=0}^{\infty} (-1)^k \Delta^{2k} v_{2k}(t) \quad (\text{A5})$$

with  $v_{2k}(t)$  satisfying the integral recurrence relation

$$v_{2k}(t) = \int_0^t dt_{2k} \exp \left( -2 \frac{t_{2k}}{T} \right) S(t_{2k}) \int_0^{t_{2k}} dt_{2k-1} \\ \times \exp \left( 2 \frac{t_{2k-1}}{T} \right) S(t_{2k-1}) v_{2k-2}(t_{2k-1}), \quad (\text{A6})$$

and  $v_0(t) = 1$ . We can transform Eq. (A6) into an algebraic recurrence relation by using the properties of Laplace transforms<sup>34</sup>

$$\tilde{v}_{2k}(p) = \int_0^{\infty} e^{-pt} v_{2k}(t) dt. \quad (\text{A7})$$

The free induction signal  $v_F(t)$  [Eq. (17)] is obtained by setting  $S(t) = 1$  for all times. Then Eq. (A6) becomes

$$\tilde{v}_{2k}(p) = \frac{1}{p(p + 2T^{-1})} \tilde{v}_{2k-2}(p), \quad (\text{A8})$$

and the Laplace transform of  $v_F(t)$  is easily calculated to be

$$\tilde{v}_F(p) = \frac{p + 2T^{-1}}{p(p + 2T^{-1}) + \Delta^2}. \quad (\text{A9})$$

The inverse transform of this expression can be obtained by expanding in partial fractions<sup>34</sup>

$$v_F(t) = \exp \left( -\frac{t}{T} \right) \left[ \frac{1}{RT} \sinh(Rt) + \cosh(Rt) \right], \quad (\text{A10})$$

where  $R^2 = T^{-2} - \Delta^2$ . We now turn to the  $\pi/2 - \pi$  echo  $v_E(t)$ , which is obtained by setting the echo function to

$$S(t) = 1 - 2\theta(t - \tau). \quad (\text{A11})$$

Then Eq. (A6) becomes

$$\tilde{v}_{2k}(p) = \frac{1}{p(p + 2T^{-1})} \left[ \tilde{v}_{2k-2}(p) - 2 \exp(-p\tau) \right. \\ \left. \times \exp(-2\tau T^{-1}) \int_0^{\tau} dt' \exp(2t' T^{-1}) v_{2k-2}(t') \right] \quad (\text{A12})$$

and after summing the series we get

$$\tilde{v}(p) = \frac{p + 2T^{-1}}{\Delta^2 + p(p + 2T^{-1})} + \frac{2\Delta^2 \exp(-p\tau)}{\Delta^2 + p(p + 2T^{-1})} f(\tau), \quad (\text{A13})$$

$$f(\tau) = \exp(-2\tau T^{-1}) \int_0^{\tau} dt' \exp(2t' T^{-1}) v_F(t'). \quad (\text{A14})$$

Using Eq. (A10), the inverse transform becomes

$$v(t) = v_F(t) + \theta(t - \tau) \frac{2\Delta^2}{R^2} \exp(-tT^{-1}) \\ \times \sinh(R\tau) \sinh[R(t - \tau)] \quad (\text{A15})$$

$$= \theta(\tau - t) v_F(t) + \theta(t - \tau) v_E(t), \quad (\text{A16})$$

which after rearrangement leads to Eq. (18) for  $t > \tau$ ,

$$v_E(t) = R^{-2} \exp(-tT^{-1}) \{ T^{-2} \cosh(Rt) + RT^{-1} \sinh(Rt) \\ - \Delta^2 \cosh[R(t - 2\tau)] \}. \quad (\text{A17})$$

## APPENDIX B: EQUIVALENCE OF ENSEMBLE $\pi/2 - \pi$ ECHO ENVELOPE AND AVERAGE SINGLE SPIN DYNAMICS

Equation (15) was derived by averaging  $\sigma_{nm}(t=0)$ , which clearly applies only to an ensemble of spins. Therefore an interesting question is how the single spin off diagonal density matrix element  $\langle S_{\perp} \rangle$  [analogous to Eq. (12), the in-plane magnetization in the  $S_z$  basis but without  $\sigma_{nm}(0)$  average] behaves under nuclear dynamics average only. The result is that the modulus squared of this quantity is exactly equal to the  $\pi/2 - \pi$  echo envelope, as we show below. The evolution under Eq. (9) is given by



$$\langle S_{\perp}(t) \rangle = \prod_{n < m} \left\langle \exp \left[ i \Delta_{nm} \int_0^t (-1)^{N_{nm}(t')} dt' \right] \right\rangle, \quad (\text{B1})$$

where  $N_{nm}(t)$  are independent Poisson random variables representing the nuclear dynamics, on which the average is taken. Using the same methods of Appendix A, it is easy to show that the argument of the product (B1) is given by

$$\begin{aligned} S_{nm}^{\perp}(t) &= \left\langle \cos \left[ \Delta_{nm} \int_0^t (-1)^{N_{nm}(t')} dt' \right] \right\rangle \\ &+ \left\langle \sin \left[ \Delta_{nm} \int_0^t (-1)^{N_{nm}(t')} dt' \right] \right\rangle \\ &= v_{nm}^{(F)}(t) + i \frac{\Delta_{nm}}{R_{nm}} \exp \left( -\frac{t}{T_{nm}} \right) \sinh(R_{nm}t), \quad (\text{B2}) \end{aligned}$$

where  $v_{nm}^{(F)}(t)$  is the free induction decay derived above [Eq. (17)]. Clearly the difference between a single spin and an ensemble is the presence of the complex term in Eq. (B2),

which leads to strong interference effects when the product over pairs is taken. To see this, we calculate

$$\begin{aligned} |S_{nm}^{\perp}(t)|^2 &= [v_{nm}^{(F)}(t)]^2 + \frac{\Delta_{nm}^2}{R_{nm}^2} \exp \left( -\frac{2t}{T_{nm}} \right) \sinh^2(R_{nm}t) \\ &= v_{nm}^{(E)}(2t). \quad (\text{B3}) \end{aligned}$$

Therefore the effect of this complex part is to enhance the coherence of the single spin, making it exactly equal to the  $\pi/2 - \pi$  echo envelope

$$|\langle S_{\perp}(\tau) \rangle|^2 = v_E(2\tau). \quad (\text{B4})$$

Notice that if we performed the product over pairs without this complex part,  $S_{\perp}$  would decay similarly to free induction  $v_F(t)$ . Many authors define a coherence time  $\tau_c$  equal to the  $1/e$  decay of the modulus of the off diagonal density matrix. If the echo is dominated by Gaussian SD, we simply have  $\tau_c = T_M/4^{1/3}$ .

- 
- <sup>1</sup>D. Loss and D.P. DiVincenzo, Phys. Rev. A **57**, 120 (1998); G. Burkard, D. Loss, and D.P. DiVincenzo, Phys. Rev. B **59**, 2070 (1999); X. Hu and S. Das Sarma, Phys. Rev. A **61**, 062301 (2000); X. Hu and S. Das Sarma, *ibid.* **64**, 042312 (2001).
- <sup>2</sup>R. Vrijen *et al.* Phys. Rev. A **62**, 012306 (2000); B.E. Kane, Fortschr. Phys. **48**, 1023 (2000).
- <sup>3</sup>B.E. Kane, Nature (London) **393**, 133 (1998); D. Mozysky, V. Privman, and M.L. Glasser, Phys. Rev. Lett. **86**, 5112 (2001).
- <sup>4</sup>S. Das Sarma, J. Fabian, X. Hu, and I. Žutić, Solid State Commun. **119**, 207 (2001); S. Das Sarma, J. Fabian, X. Hu, and I. Žutić, IEEE Trans. Magn. **36**, 2821 (2000).
- <sup>5</sup>J. Preskill, Proc. R. Soc. London, Ser. A **454**, 385 (1998).
- <sup>6</sup>R. de Sousa and S. Das Sarma, Phys. Rev. B **67**, 033301 (2003).
- <sup>7</sup>X. Hu, R. de Sousa, and S. Das Sarma, cond-mat/0108339 (unpublished); (unpublished).
- <sup>8</sup>A. Abragam, *The Principles of Nuclear Magnetism* (Oxford University Press, London, 1961); C.P. Slichter, *Principles of Magnetic Resonance* (Springer-Verlag, Berlin, 1996); C.P. Poole and H.A. Farach, *Relaxation in Magnetic Resonance* (Academic Press, New York, 1971).
- <sup>9</sup>W.B. Mims, in *Electron Paramagnetic Resonance*, edited by S. Geschwind (Plenum Press, New York, 1972).
- <sup>10</sup>B. Herzog and E.L. Hahn, Phys. Rev. **103**, 148 (1956).
- <sup>11</sup>J.R. Klauder and P.W. Anderson, Phys. Rev. **125**, 912 (1962).
- <sup>12</sup>G.M. Zhidomirov and K.M. Salikhov, Sov. Phys. JETP **29**, 1037 (1969).
- <sup>13</sup>G. Feher, Phys. Rev. **114**, 1219 (1959).
- <sup>14</sup>G. Feher and E.A. Gere, Phys. Rev. **114**, 1245 (1959).
- <sup>15</sup>D.K. Wilson and G. Feher, Phys. Rev. **124**, 1068 (1961).
- <sup>16</sup>H. Hasegawa, Phys. Rev. **118**, 1523 (1960); L.M. Roth, *ibid.* **118**, 1534 (1960).
- <sup>17</sup>M. Chiba and A. Hirai, J. Phys. Soc. Jpn. **33**, 730 (1972).
- <sup>18</sup>A.M. Tyryshkin, S.A. Lyon, A.V. Astashkin, and A.M. Raitsimring, cond-mat/0303006 (unpublished).
- <sup>19</sup>A.A. Kiselev, E.L. Ivchenko, and U. Rössler, Phys. Rev. B **58**, 16 353 (1998).
- <sup>20</sup>A.V. Khaetskii and Y.V. Nazarov, Phys. Rev. B **64**, 125316 (2001); L.M. Woods, T.L. Reinecke, and Y. Lyanda-Geller, *ibid.* **66**, 161318(R) (2001).
- <sup>21</sup>A.V. Khaetskii, D. Loss, and L. Glazman, Phys. Rev. Lett. **88**, 186802 (2002); S. Saykin, D. Mozysky, and V. Privman, Nano Lett. **2**, 651 (2002).
- <sup>22</sup> $v(2\tau)$  was derived for  $T_1$  samples by G.M. Zhidomirov and K.M. Salikhov: (Ref. 12) however, their formulas have a misprint: In their Eq. (11),  $T_1^{-2} \sinh(R\tau)$  should read  $T_1^{-2} \sinh^2(R\tau)$ .
- <sup>23</sup>J.H. Van Vleck, Phys. Rev. **74**, 1168 (1948).
- <sup>24</sup>N. Bloembergen, S. Shapiro, P.S. Pershan, and J.O. Artman, Phys. Rev. **114**, 445 (1959).
- <sup>25</sup>*CRC Handbook of Chemistry and Physics*, 70th ed. (CRC Press, Boca Raton, Florida, 1989).
- <sup>26</sup>W. Kohn, *Solid State Physics*, (1957) vol. 5, p. 257.
- <sup>27</sup>R.G. Shulman and B.J. Wyluda, Phys. Rev. **103**, 1127 (1956).
- <sup>28</sup>J.P. Gordon and K.D. Bowers, Phys. Rev. Lett. **1**, 368 (1958).
- <sup>29</sup>L.M.K. Vandersypen *et al.*, quant-ph/0207059 (unpublished).
- <sup>30</sup>B. Koiller, X. Hu, and S. Das Sarma, Phys. Rev. Lett. **88**, 027903 (2002).
- <sup>31</sup>M. Seck, M. Potemski, and P. Wyder, Phys. Rev. B **56**, 7422 (1997).
- <sup>32</sup>H.-A. Engel and D. Loss, Phys. Rev. Lett. **86**, 4648 (2001).
- <sup>33</sup>D. Paget, G. Lampel, B. Sapoval, and V.I. Safarov, Phys. Rev. B **15**, 5780 (1977).
- <sup>34</sup>G.B. Arfken and H.J. Weber, *Mathematical Methods for Physicists*, 4th Ed. (Academic Press, London, 1995).
- <sup>35</sup>A.M. Tyryshkin and S.A. Lyon (private communication).
- <sup>36</sup>D. Mozysky, Sh. Kogan, V.N. Gorshkov, and G.P. Berman, Phys. Rev. B **65**, 245213 (2002).
- <sup>37</sup>C. Tahan, M. Friesen, and R. Joynt, Phys. Rev. B **66**, 035314 (2002).